Ionics (2013) 19:1207–1213
DOI 10.1007/s11581-013-0955-5

SHORT COMMUNICATION

Preparation of PdAu/C-Sb_2O_5·SnO_2 electrocatalysts by borohydride reduction process for direct formic acid fuel cell

**J. Nandenha · R. F. B. De Souza · M. H. M. T. Assumpção ·
E. V. Spinacé · A. O. Neto**

Received: 27 March 2013 / Revised: 17 June 2013 / Accepted: 29 June 2013 / Published online: 24 July 2013

Abstract Pd/C-Sb_2O_5·SnO_2 and PdAu/C-Sb_2O_5·SnO_2 electrocatalysts with different PdAu atomic ratio (90:10, 70:30, and 50:50) were prepared by borohydride reduction method, and characterized by X-ray diffraction, transmission electron microscopy, cyclic voltammetry, chronoamperommetry, and performance test on direct formic acid fuel cell at 100 °C. X-ray diffraction showed for Pd/C-Sb_2O_5·SnO_2 the presence of Pd face-centered cubic (fcc) system, while for PdAu/C-Sb_2O_5·SnO_2 it showed the presence of Pd fcc phase, PdAu fcc alloys and a segregated phases fcc Pd-rich and Au-rich phases. TEM micrographs and histograms for all electrocatalysts showed that the nanoparticles where not well dispersed on the support and some agglomerates were present. The electrochemical studies showed that PdAu/C-Sb_2O_5·SnO_2 (70:30) had superior performance for formic acid electro-oxidation at 25 °C compared to others electrocatalysts prepared while PdAu/C-Sb_2O_5·SnO_2 (90:10) showed superior performance in direct formic acidic fuel cell at 100 °C. These results indicated that the addition of 10–30 % Au to Pd favor the electro-oxidation of formic acid. This effect could be attributed to the synergy between the constituents of the electrocatalyst (metallic Pd and Au, SnO_2, and Sb_2O_5·SnO_2).

Keywords PdAu/C-Sb_2O_5·SnO_2 electrocatalysts · Formic acid oxidation · Fuel cell · Borohydride reduction process

---

J. Nandenha · R. F. B. De Souza · M. H. M. T. Assumpção ·
E. V. Spinacé · A. O. Neto (✉)
Instituto de Pesquisas Energéticas e Nucleares—IPEN-CNEN/SP,
Cidade Universitária, Av. Prof. Lineu Prestes, 2242, 05508-900 São Paulo, São Paulo, Brazil
e-mail: aolivei@ipen.br

Introduction

Fuel cells are electrochemical devices that convert chemical energy directly into electrical energy with high efficiency and low or none pollutant emission [1, 2]. The use of hydrogen as a fuel has shown higher current densities; however, the hydrogen still presents problems of production, storage, and delivery [3, 4]. Thus, the use of a liquid as fuel has been considering very attractive as power sources for stationary, mobile, and portable applications [5].

Methanol has been the fuel most studied for polymer electrolyte membrane fuel cells due to their low cost, low pollutant emissions, and high theoretical energy density [6]. However, the use of methanol as fuel has some disadvantages: (1) it is easy to penetrate through the Nafion® membrane causing the decrease in fuel cell performance; (2) Pt, usually used as the anodic catalyst, is easy to be poisoned with CO, an intermediate of the methanol oxidation; and (3) the use of methanol is not safe because methanol is a toxic, evaporable, and burnable compound.

Therefore, formic acid has been proposed as an alternative to methanol because it is non-toxic, not inflammable, and thus its storage and transportation are safe [7]. Formic acid also has shown two orders of magnitude smaller crossover flux through a Nafion® membrane than methanol [7, 8].

Considering the electro-oxidation of formic acid, Pt electrocatalyst has commonly been used. However, Pt alone is not a good catalyst because it is easily poisoned by CO. Thus, the development of new electrocatalyst is still necessary [9, 10].

Pd electrocatalyst has been able to catalyze formic acid oxidation and it is less inclined to CO poisoning and deactivation in comparison with Pt. However, the catalytic activity and durability of Pd catalysts still need to be substantially improved, consequently the addition of co-catalysts to palladium is necessary [10–12].

Chiou [13] showed that Au (10 wt%)/[Pd/multi-walled carbon nanotube (MWCNTs) (1:9)] catalyst exhibits higher activity and better stability than that of Pd/MWCNTs electrocatalyst in formic acid electro-oxidation during cyclic voltammetric experiments. This author showed that Au improves considerably the performance of Pd-based catalysts in electrochemical reaction and that the hybrid Pd–Au/MWCNTs materials could have a potential to be used in the direct formic acidic fuel cell (DFAFC).

Lu [14] has shown that the incorporation of Cu also greatly improves the electrocatalytic stability of the Pd/C catalysts and the atomic ratio of Pd and Cu also has a great influence on the enhancement of the electrocatalytic stability, where the Pd_3Cu_1/C catalyst showed the best electrocatalytic stability for formic acid oxidation, in comparison to another atomic ratio of Pd on Cu.

The addition of metal oxides into noble metal can enhance the catalytic activity toward small organic molecule electro-oxidation synergetic interaction metal oxides and noble metals. Among those, antimony tin oxide ($Sb_2O_5 \cdot SnO_2$) exhibits a number of characteristics that make them interesting for catalytic studies due to enhancement of electrical conductivity compared with others oxides. Moreover, the presence of ATO oxides could also be beneficial to the oxidation of some poisoning intermediates adsorbed (bifunctional mechanism) [15, 16].

Oliveira Neto et al. [17] showed that Pt nanoparticles supported on a physical mixture of carbon and ATO were more active for ethanol oxidation in acidic medium compared to Pt nanoparticles supported only on ATO or on carbon. The enhancement of activity was attributed to better dispersion of Pt particles on the ATO support, as well as to the effects of SnO_2 adjacent to Pt (bifunctional effect and/or the electronic effect) [17, 18]

In this context, the aim of this work was prepare PdAu/C-$Sb_2O_5 \cdot SnO_2$ electrocatalysts by borohydride reduction and test these electrocatalyst for formic acid electro-oxidation in acidic medium by cyclic voltammetry, chronoamperometry, and in a single DFAFC.

Experimental

PdAu/C-$Sb_2O_5 \cdot SnO_2$ (20 wt% of metals loading, with Pd/Au atomic ratio of 90:10, 70:30, and 50:50) were prepared by borohydride reduction method using $HAuCl_4 \cdot 3H_2O$ and $Pd(NO_3)_2 \cdot 2H_2O$ (Aldrich) as metal sources, sodium borohydride as reducing agent and a physical mixture of 85 % Vulcan Carbon XC72 and 15 % $Sb_2O_5 \cdot SnO_2$ as support. Initially, the metal sources were dissolved in a mixture of water/2-propanol (50:50, *v/v*), while the support was dispersed in the solution. The resulting mixture was submitted to an ultrasonic bath for 5 min. After this, a solution of sodium borohydride was added under stirring in one portion at room temperature. Finally, the obtained solid was filtered, washed with water and dried at 70 °C for 2 h [16].

X-ray diffraction (XRD) analyses were performed in a RigaKu Miniflex II diffractometer using Cu Kα radiation source (λ=0.15406 nm). The diffractograms were recorded from 2θ=20° to 90° with a step size of 0.05° and a scan time of 2 s per step. Transmission electron microscopy (TEM) was carried out using a JEOL JEM-2100 electron microscope operated at 200 kV. Mean particle sizes were determined by counting more than 200 particles from different regions of each sample.

The cyclic voltammetry and chronoamperommetry measurements were carried out at 25 °C using a Microquímica (model MQPG01, Brazil) potentiostat/galvanostat.

These study were performed using a working electrodes (geometric area of 0.3 cm^2 with a depth of 0.3 mm) prepared by thin porous coating technique [18], the reference electrode was a reversible hydrogen electrode (RHE) and the counter electrode was a Pt plate. The electrochemical measurements were realized in presence of 0.5 mol L^{-1} H_2SO_4 or 1.0 mol L^{-1} of formic acid+0.5 mol L^{-1} H_2SO_4 solutions saturated with N_2.

Direct formic acid fuel cell tests were performed using Pd/C-$Sb_2O_5 \cdot SnO_2$ or PdAu/C-$Sb_2O_5 \cdot SnO_2$ electrocatalysts as anode and Pt/C electrocatalysts as cathode in a single cell with an area of 5 cm^2. For direct formic acid fuel cell studies it was also utilized the carbon-cloth teflon-treated as a gas diffusion layer and a Nafion 117® membrane as electrolyte. The electrodes (anode or cathode) were hot pressed on both sides of a Nafion® 117 membrane at 100 °C for 2 min under a pressure of 225 kgf cm^{-2}. The electrodes prepared contain 1 mg Pd cm^{-2} in the anode. The temperature was set to 100 °C for the fuel cell and 80 °C for the oxygen humidifier, 8 mol L^{-1} formic acid aqueous solution was delivered at approximately 1 mL min^{-1} and the oxygen flow was set to 500 mL min^{-1} under 2 bar of pressure.

Results and discussion

The X-ray diffractograms of Pd/C-$Sb_2O_5 \cdot SnO_2$ and PdAu/C-$Sb_2O_5 \cdot SnO_2$ electrocatalysts are shown in Fig. 1. All electrocatalysts prepared showed a broad peak at about 2θ=25° associated to the carbon support material and peaks at about 2θ=27°, 34°, 38°, 52°, 55°, 62°, 65°, and 66°, which were also characteristic of ATO used as support [15]. The Pd/C-$Sb_2O_5 \cdot SnO_2$ and PdAu/C-$Sb_2O_5 \cdot SnO_2$ electrocatalysts also presented five peaks at about 2θ=40°, 47°, 68°, 82°, and 87° associated, respectively, to (111), (200), (220), (311),

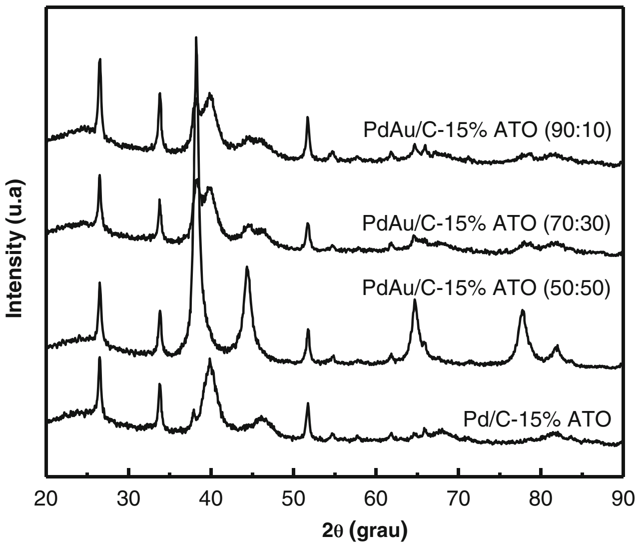

Fig. 1 X-ray diffractograms of the Pd/C-$Sb_2O_5·SnO_2$ and PdAu/C-$Sb_2O_5·SnO_2$ electrocatalysts

and (222) planes of face-centered cubic (fcc) structure of Pd or Pd alloys.

All PdAu/C-$Sb_2O_5·SnO_2$ electrocatalysts also showed a shift to smaller angles of the peak associated to the (220) plane compared to Pd/C electrocatalyst with the increasing Au content. This result indicated the insertion of Au in the Pd structure. For PdAu/C-$Sb_2O_5·SnO_2$ (90:10) and PdAu/C-$Sb_2O_5·SnO_2$ (70:30) was also observed a segregated of fcc Pd-rich and Au-rich phases about $2\theta=38°$ and 40°, respectively. This result was also observed in previous work [13, 19].

TEM micrographs and histograms of the particle size distributions of PdAu/C-$Sb_2O_5·SnO_2$ electrocatalysts are shown in Fig. 2. All images showed that the nanoparticles where not well dispersed on the support and some agglomerates were present. The mean particle sizes of Pd/C-$Sb_2O_5·SnO_2$, PdAu/C-$Sb_2O_5·SnO_2$ (90:10), PdAu/C-$Sb_2O_5·SnO_2$ (70:30), and PdAu/C-$Sb_2O_5·SnO_2$ (50:50) electrocatalysts were 6.4, 6.6, 6.7, and 7.4 nm, respectively. The increase of Au content in PdAu/C electrocatalysts resulted in an increase of mean particle size, confirmed to XRD. This behavior has also been observed by Brandalise [19].

Chiou [13] showed that the metal nanoparticles in Au–Pd/MWCNTs are larger than those in Pd/MWCNTs, where the amount of Au increases leads to an increase in the particle size making them more agglomerated with particle size about 10–30 nm. Brandalise [19] and Zhu [20] explained that Au is nobler than Pd and then reduces forming Au seeds, while Pd grows epitaxially on its surface rather than Au forming a new nucleus.

The cyclic voltammograms of Pd/C-$Sb_2O_5·SnO_2$ and PdAu/C-$Sb_2O_5·SnO_2$ electrocatalysts in 0.5 mol L^{-1} H_2SO_4 solution are shown in Fig. 3. The Pd/C-$Sb_2O_5·SnO_2$, PdAu/C-$Sb_2O_5·SnO_2$ (90:10), and PdAu/C-$Sb_2O_5·SnO_2$ (70:30) electrocatalysts showed a well-defined hydrogen adsorption–desorption region (peaks in the range of 0.05 to 0.35 V vs RHE). The voltammograms of PdAu/C-$Sb_2O_5·SnO_2$ (50:50) is suppressed in comparison with others electrocatalysts prepared indicating partial coverage of Pd by Au.

All PdAu/C-$Sb_2O_5·SnO_2$ electrocatalysts also showed the clear shifts of the peak positions for the hydrogen adsorption–desorption in comparison with Pd/C-$Sb_2O_5·SnO_2$. This negative shift is an indication of the electronic modification of Pd atoms by the neighboring Au atoms [21].

For PdAu/C-$Sb_2O_5·SnO_2$ (70:30) and PdAu/C-$Sb_2O_5·SnO_2$ (50:50), we observed an increase in the current values in the double layer (0.4–0.8 V) in comparison with Pd/C-$Sb_2O_5·SnO_2$ and PdAu/C-$Sb_2O_5·SnO_2$ (90:10), indicating more formation of Pd and Au oxide species. The negative scan also showed an increase in the currents in the double layer at about 0.55 V that could be associated with the reduction of oxide species presents in the electrocatalyst. The capacitance increase could also be explained by the potential decrease of palladium that is normally 0.6 V vs RHE (or 0.43 V vs Ag /AgCl) as a reported by Yang [22], due to the presence of Au that is nobler than Pd providing OH and O species at less positive potential, as already described by Germain [23]. This effect was most pronounced at PdAu/C-$Sb_2O_5·SnO_2$ (50:50) because of the highest Au content. However, the capacitance increases with Au content.

Figure 4 shows the cyclic voltammograms of Pd/C-$Sb_2O_5·SnO_2$ and PdAu/C-$Sb_2O_5·SnO_2$ electrocatalysts prepared at 25 °C in the presence of 1.0 mol L^{-1} formic acidic in 0.5 mol L^{-1} H_2SO_4. PdAu/C-$Sb_2O_5·SnO_2$ (70:30) showed the highest current values in all potential range in comparison with others electrocatalysts prepared; however, PdAu/C-$Sb_2O_5·SnO_2$ (90:10) and Pd/C-$Sb_2O_5·SnO_2$ showed similar performance in all potential range, while PdAu/C-$Sb_2O_5·SnO_2$ (50:50) showed lower currents values in comparison to the others electrocatalysts for potentials above of 0.4 V.

The enhancement of formic acid electro-oxidation on PdAu/C-$Sb_2O_5·SnO_2$ (70:30) could be caused by the changed reaction pathway due to ensemble effect or by the effective removal of CO_{ads} formed in the dehydration path resulted from the electronic effect of Au donating electrons to the d-band of Pd [13].

Chiou [13] also showed that Au (10 wt%)/[Pd/MWCNTs-(1:9)] catalyst exhibits higher activity and better stability than that of Pd/MWCNTs catalyst in formic acid electro-oxidation. These authors concluded that Au improved considerably the performance of Pd-based catalysts in electrochemical reaction because the Au (10 wt%)/[Pd/MWCNTs (1:9)] converted 100 % of CO to CO_2 and its CO conversion performance was due to the presence of Pd (10 wt%)/MWCNTs and Au (10 wt%)/MWCNTs.

Figure 5 shows the current–time curves for formic acidic electro-oxidation for Pd/C-$Sb_2O_5·SnO_2$ and PdAu/C-$Sb_2O_5·SnO_2$ electrocatalysts at 25 °C in the potential of 0.5 V for 30 min.

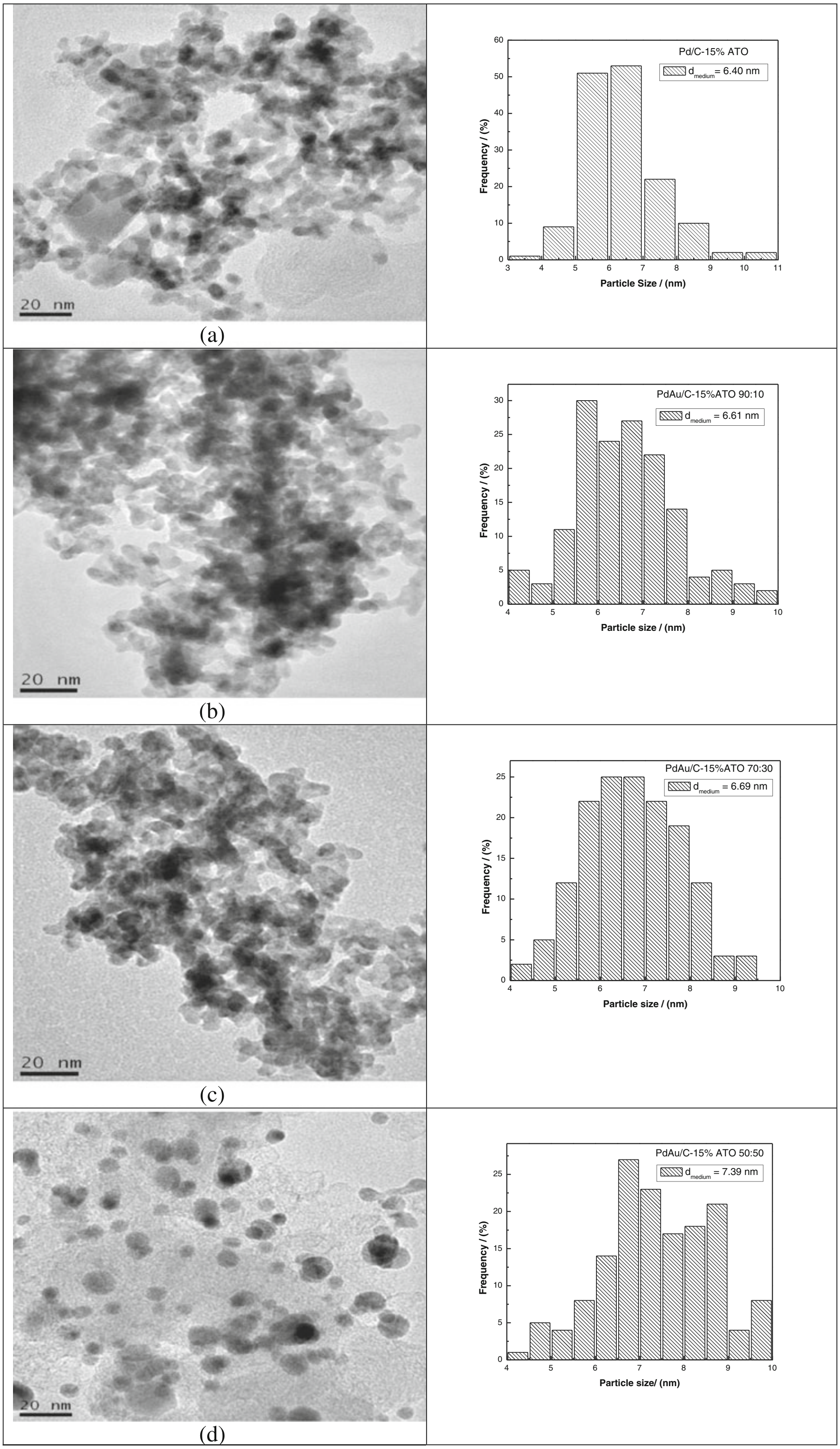

Fig. 2 TEM micrograph and a histogram of **a** Pd/C-$Sb_2O_5 \cdot SnO_2$, **b** PdAu/C-$Sb_2O_5 \cdot SnO_2$ (90:10), **c** PdAu/C-$Sb_2O_5 \cdot SnO_2$ (70:30), and **d** PdAu/C-$Sb_2O_5 \cdot SnO_2$ (50:50) electrocatalyst with the mean diameter and particle distribution

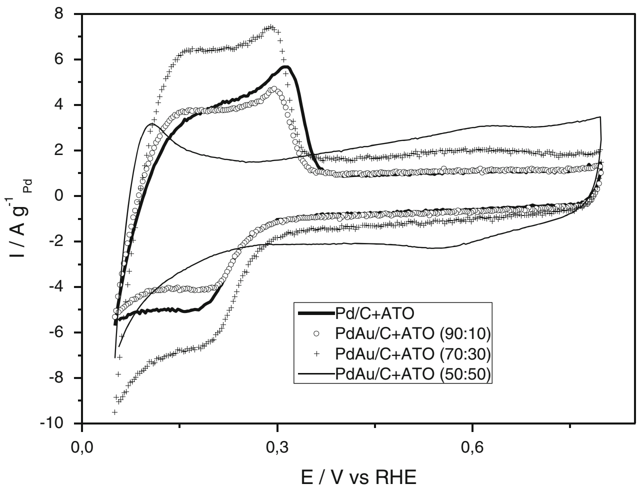

Fig. 3 Cyclic voltammograms of Pd/C-Sb_2O_5·SnO_2 and PdAu/C-Sb_2O_5·SnO_2 electrocatalysts in 0.5 mol L^{-1} H_2SO_4 with a sweep rate of 10 mV s^{-1}

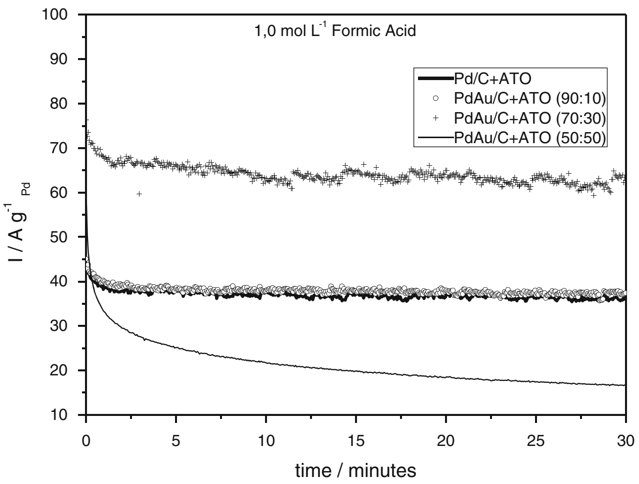

Fig. 5 Current–time curves at 0.5 V in 1 mol L^{-1} formic acid solution in 0.5 mol L^{-1} H_2SO_4 for Pd/C-Sb_2O_5·SnO_2 and PdAu/C-Sb_2O_5·SnO_2 electrocatalysts at 25 °C

The current values obtained for PdAu/C-Sb_2O_5·SnO_2 (70:30) were higher than those obtained for PdAu/C-Sb_2O_5·SnO_2 (90:10), Pd/C-Sb_2O_5·SnO_2, and PdAu/C-Sb_2O_5·SnO_2 (50:50) in agreement with cyclic voltammetry experiments. The final current values at 0.5 V (T=25 °C) increase in the following order: PdAu/C-Sb_2O_5·SnO_2 (70:30)>PdAu/C-Sb_2O_5·SnO_2 (90:10)>Pd/C-Sb_2O_5·SnO_2>PdAu/C-Sb_2O_5·SnO_2 (50:50).

All of the catalysts featured a pronounced current decay in the first 2 min due to the accumulation of poisonous intermediates and the current values of PdAu/C-Sb_2O_5·SnO_2 (50:50) decay slowed down at longer times. The activity of PdAu/C-Sb_2O_5·SnO_2 (70:30) was 1.7 times of the Pd/C-Sb_2O_5·SnO_2 indicating that the activity and stability of Pd could be significantly improved due to the co-presence of Au. The electronic modification of Pd might be the possible reasons for the enhanced activity, as the proximity of Au and Pd atoms on the surface of the C-Sb_2O_5·SnO_2 (bifunctional mechanism) [24].

Figure 6 shows the performances of a single DFAFC using Pd/C-Sb_2O_5·SnO_2 and PdAu/C-Sb_2O_5·SnO_2 electrocatalysts as anode electrocatalysts.

PdAu/C-Sb_2O_5·SnO_2 (90:10) electrocatalysts showed higher values of maximum power density (61 mW cm^{-2}) in comparison with Pd/C-Sb_2O_5·SnO_2 (56 mW cm^{-2}), PdAu/C-Sb_2O_5·SnO_2 (70:30) (52 mW cm^{-2}), and PdAu/C-Sb_2O_5·SnO_2 (50:50) (43 mW cm^{-2}). The experiments at 100 °C on single DFAFC also showed that the addition of Au into Pd/C-Sb_2O_5·SnO_2 electrocatalyst can promote its activity for formic acidic electro-oxidation.

A Pt/C electrocatalyst was also used for comparison with Pd/C-Sb_2O_5·SnO_2, Pd/C-Sb_2O_5·SnO_2 electrocatalyst showed

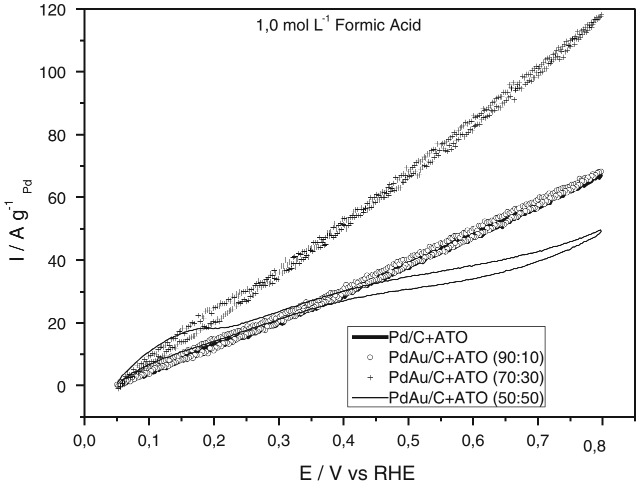

Fig. 4 Cyclic voltammograms of the Pd/C-Sb_2O_5·SnO_2 and PdAu/C-Sb_2O_5·SnO_2 electrocatalysts in 1 mol L^{-1} formic acid solution in 0.5 mol L^{-1} H_2SO_4 with a sweep rate of 10 mV s−^{1} at 25 °C

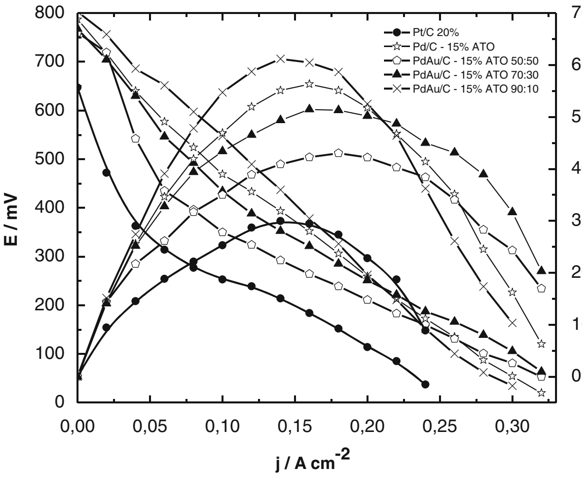

Fig. 6 I–V curves and the power density at 100 °C of a 5 cm^2 DFAFC using Pd/C-Sb_2O_5·SnO_2 and PdAu/C-Sb_2O_5·SnO_2 electrocatalysts

a higher values of maximum power density in comparison with Pt/C (30 mW cm^{-2}) indicating that the use of palladium and C-$Sb_2O_5 \cdot SnO_2$ for formic acid electro-oxidation is more appropriated, since the presence of $Sb_2O_5 \cdot SnO_2$ could enhance the formation of chemisorbed oxygen species that promotes the oxidation of adsorbed carbon monoxide or intermediate adsorbed on the surface of palladium.

Choi [25] showed that an unsupported PtAu alloy prepared by borohydride reduction as anode catalyst for DFAFC had a higher catalytic activity in comparison with Pt/C and PtRu/C. These authors concluded that the oxidation of formic acid on a Pt–Au catalyst occurs mainly through the direct dehydrogenation pathway, without significant formation of adsorbed CO, while Chiou [13] has shown that the initial power density of the PdAu/MWCNTs was higher than that for the Pd/MWCNTs; however, PdAu/MWCNTs deactivates due to the formation of poisons from impurities of formic acid. These authors concluded that the performance of PdAu electrocatalysts for formic acid oxidation strongly depends on the catalyst preparation method and the effect of adding various amounts of Auto MWCNTs-supported Pd electrocatalyst.

The highest catalytic activity of PdAu/C-$Sb_2O_5 \cdot SnO_2$ (70:30) and PdAu/C-$Sb_2O_5 \cdot SnO_2$ (90:10) prepared by borohydride reduction process could be attributed to the synergy between the constituents of the electrocatalyst (metallic Pd and Au, SnO_2, and $Sb_2O_5 \cdot SnO_2$), thus, the presence of $Sb_2O_5 \cdot SnO_2$ could enhance the formation of chemisorbed oxygen species which promotes the oxidation of adsorbed carbon monoxide and/or intermediates species adsorbed on the surface of Pd. The enhancement of formic acid electro-oxidation on PdAu/C-$Sb_2O_5 \cdot SnO_2$ could be caused by the changed reaction pathway due to ensemble effect or by the effective removal of CO_{ads} formed in the dehydration path resulted from the electronic effect of Au donating electrons to the d-band of Pd [13].

Conclusion

The borohydride reduction method was an efficient process to produce Pd/C-$Sb_2O_5 \cdot SnO_2$ and PdAu/C-$Sb_2O_5 \cdot SnO_2$ electro catalysts for formic acid electro-oxidation. The PdAu/C-$Sb_2O_5 \cdot SnO_2$ electrocatalysts obtained showed the presence of PdAu (fcc) alloys, a segregated fcc Pd-rich and Au-rich phases and ATO oxide phases. The electrochemical measurements and the experiments in a single DFAFC showed that PdAu/C-$Sb_2O_5 \cdot SnO_2$ (70:30) and PdAu/C-$Sb_2O_5 \cdot SnO_2$ (90:10) exhibited superior performance for formic acid electro-oxidation than Pd/C-$Sb_2O_5 \cdot SnO_2$ electrocatalysts. The highest catalytic activity of PdAu/C-$Sb_2O_5 \cdot SnO_2$ (70:30) could be attributed to the synergy between the constituents of the electrocatalyst (metallic Pd and Au, SnO_2, and $Sb_2O_5 \cdot SnO_2$). Further work is now necessary to investigate the electrocatalyst surface and to elucidate the mechanism of formic acid electro-oxidation using these electrocatalysts.

Acknowledgments The authors thank the Laboratório de Microscopia do Centro de Ciências e Tecnologia de Materiais (CCTM) by TEM measurements, FAPESP (2011/18246-0, 2012/03516-5), and CNPq (150639/2013-9) for the financial support.

References

1. Tusi MM, Polanco NSO, Brandalise M, Correa OV, Silva AC, Ribeiro VA, Neto AO, Spinace EV (2012) PtRu/carbon hybrid materials prepared by hydrothermal carbonization as electrocatalysts for methanol electrooxidation. Ionics 18(1–2):215
2. Mekhilef S, Saidur R, Safari A (2012) Comparative study of different fuel cell technologies. Renew Sustain Energ Rev 16(1):981
3. Balat M (2008) Potential importance of hydrogen as a future solution to environmental and transportation problems. Int J Hydrogen Energ 33(15):4013
4. Vigier F, Rousseau S, Coutanceau C, Leger JM, Lamy C (2006) Electrocatalysis for the direct alcohol fuel cell. Top Catal 40(1–4):111
5. Zhou WJ, Zhou B, Li WZ, Zhou ZH, Song SQ, Sun GQ, Xin Q, Douvartzides S, Goula M, Tsiakaras P (2004) Performance comparison of low-temperature direct alcohol fuel cells with different anode catalysts. J Power Sources 126(1–2):16
6. Kadirgan F, Beyhan S, Atilan T (2009) Preparation and characterization of nano-sized Pt–Pd/C catalysts and comparison of their electro-activity toward methanol and ethanol oxidation. Int J Hydrogen Energ 34(10):4312
7. Wang X, Tang Y, Gao Y, Lu T (2008) Carbon-supported Pd-Ir catalyst as anodic catalyst in direct formic acid fuel cell. J Power Sources 175(2):784
8. Rhee Y-W, Ha SY, Masel RI (2003) Crossover of formic acid through Nafion® membranes. J Power Sources 117(1–2):35
9. Jiang J, Kucernak A (2002) Nanostructured platinum as an electrocatalyst for the electrooxidation of formic acid. J Electroanal Chem 520(1–2):64
10. An H, Cui H, Zhou D, Tao D, Li B, Zhai J, Li Q (2013) Synthesis and performance of Pd/SnO2–TiO2/MWCNT catalysts for direct formic acid fuel cell application. Electrochim Acta 92:176
11. Cameron D, Holliday R, Thompson D (2003) Gold's future role in fuel cell systems. J Power Sources 118(1–2):298
12. Corti CW, Holliday RJ, Thompson DT (2007) Progress towards the commercial application of gold catalysts. Top Catal 44(1–2):331
13. Chiou YJ, Chen KY, Lin HM, Liou WJ, Liou HW, Wu SH, Mikolajczuk A, Mazurkiewicz M, Malolepszy A, Stobinski L, Borodzinski A, Kedzierzawski P, Kurzydlowski K, Chien SH, Chen WC (2011) Electrocatalytic properties of hybrid palladium-gold/multi-walled carbon nanotube materials in fuel cell applications. Phys Status Solidi A 208(8):1778–1782
14. Lu L, Shen L, Shi Y, Chen T, Jiang G, Ge C, Tang Y, Chen Y, Lu T (2012) New insights into enhanced electrocatalytic performance of carbon supported Pd–Cu catalyst for formic acid oxidation. Electrochim Acta 85:187
15. Feng L, Yao S, Zhao X, Yan L, Liu C, Xing W (2012) Electrocatalytic properties of Pd/C catalyst for formic acid electrooxidation promoted by europium oxide. J Power Sources 197:38
16. Piasentin RM, de Souza RFB, Silva JCM, Spinacé EV, Santos MC, Neto AO (2013) Electro-oxidation of Ethanol on PtPdSn/C-

$Sb_2O_5{\cdot}SnO_2$ electrocatalysts prepared by borohydride reduction. Int J Electrochem Sci 8(1):435

17. Neto AO, Brandalise M, Dias RR, Ayoub JMS, Silva AC, Penteado JC, Linardi M, Spinacé EV (2010) The performance of Pt nanoparticles supported on $Sb_2O_5{\cdot}SnO_2$, on carbon and on physical mixtures of $Sb_2O_5{\cdot}SnO_2$ and carbon for ethanol electro-oxidation. Int J Hydrogen Energ 35(17):9177
18. Castro JC, Antoniassi RM, Dias RR, Linardi M, Spinacé EV, Neto AO (2012) Preparation of PtSnRh/C-Sb 2O 5 · SnO 2 electrocatalysts by an alcohol reduction process for direct ethanol fuel cell. Ionics 18(8):781
19. Brandalise M, Tusi MM, Piasentin RM, Santos MCD, Spinacé EV, Neto AO (2012) Synthesis of PdAu/C and PdAuBi/C electrocatalysts by borohydride reduction method for ethylene glycol electro-oxidation in alkaline medium. Int J Electrochem Sci 7(10):9609
20. Zhu LD, Zhao TS, Xu JB, Liang ZX (2009) Preparation and characterization of carbon-supported sub-monolayer palladium decorated gold nanoparticles for the electro-oxidation of ethanol in alkaline media. J Power Sources 187(1):80
21. Obradović MD, Rogan JR, Babić BM, Tripković AV, Gautam ARS, Radmilović VR, Gojković SL (2012) Formic acid oxidation on Pt–Au nanoparticles: relation between the catalyst activity and the poisoning rate. J Power Sources 197:72
22. Yang F, Cheng K, Wu T, Zhang Y, Yin J, Wang G, Cao D (2013) Dendritic palladium decorated with gold by potential pulse electrodeposition: Enhanced electrocatalytic activity for H2O2 electroreduction and electrooxidation. Electrochim Acta 99:54
23. Germain PS, Pell WG, Conway BE (2004) Evaluation and origins of the difference between double-layer capacitance behaviour at Au-metal and oxidized Au surfaces. Electrochim Acta 49(11):1775
24. Feng Y-Y, Liu Z-H, Xu Y, Wang P, Wang W-H, Kong D-S (2013) Highly active PdAu alloy catalysts for ethanol electro-oxidation. J Power Sources 232:99
25. Choi J-H, Jeong K-J, Dong Y, Han J, Lim T-H, Lee J-S, Sung Y-E (2006) Electro-oxidation of methanol and formic acid on PtRu and PtAu for direct liquid fuel cells. J Power Sources 163(1):71